High magnetization and the high-temperature superparamagnetic transition with intercluster interaction in disordered zinc ferrite thin film

2005 J. Phys.: Condens. Matter 17 137

(http://iopscience.iop.org/0953-8984/17/1/013)

INSTITUTE OF PHYSICS PUBLISHING JOURNAL OF PHYSICS: CONDENSED MATTER

J. Phys.: Condens. Matter **17** (2005) 137–149 doi:10.1088/0953-8984/17/1/013

High magnetization and the high-temperature superparamagnetic transition with intercluster interaction in disordered zinc ferrite thin film

Seisuke Nakashima, Koji Fujita[1], Katsuhisa Tanaka and Kazuyuki Hirao

Department of Material Chemistry, Graduate School of Engineering, Kyoto University, Nishikyo-ku, Kyoto 615-8510, Japan

E-mail: koji@collon1.kuic.kyoto-u.ac.jp

Received 8 September 2004, in final form 1 November 2004
Published 10 December 2004
Online at stacks.iop.org/JPhysCM/17/137

Abstract

Magnetic properties have been investigated for a zinc ferrite thin film deposited on glass at a substrate temperature close to room temperature using a sputtering method. X-ray diffraction analysis reveals that the thin film consists of nanocrystalline $ZnFe_2O_4$ with the size of approximately 10 nm. The magnetization at 300 K as a function of the external magnetic field shows ferrimagnetic behaviour, and tends to be saturated to the high value of 32 emu g^{-1} when the external magnetic field is higher than 30 kOe. It is considered that the preparation of the $ZnFe_2O_4$ thin film by the sputtering method, which involves very rapid cooling of vapour to form the solid-state phase, causes the random distribution of Zn^{2+} and Fe^{3+} ions in the spinel structure. In such a situation, Fe^{3+} ions occupy both octahedral and tetrahedral sites, and the strong superexchange interaction among them gives rise to ferrimagnetic properties accompanied with high magnetization. The static and dynamic magnetic responses, such as the frequency dependence of the linear ac susceptibility, the temperature dependence of the nonlinear ac susceptibility, the discrepancy between the zero-field-cooled (ZFC) and field-cooled dc magnetizations, and the relaxation of the ZFC magnetization, demonstrate that the magnetism of the present thin film is attributable to the superparamagnetism with the interaction among magnetic clusters. Spin freezing occurs at a temperature higher than room temperature (∼325 K).

1. Introduction

Spinel-type oxides containing transition metal ions are interesting from the viewpoint of magnetism of solids because they show various magnetic properties such as paramagnetism,

[1] Author to whom any correspondence should be addressed.

0953-8984/05/010137+13$30.00

ferrimagnetism, antiferromagnetism, and spin glass or cluster spin glass behaviour [1, 2]. In spinel-type oxides with general formula AB_2O_4, the anions (O^{2-} ions) form a face-centred cubic close packing in which the interstices are occupied by four-coordinated (A) and six-coordinated (B) cations. The interaction between magnetic moments on A- and B-sites is of superexchange type via O^{2-} and results in the magnetic moments being antiparallel to each other. Since the superexchange interaction is stronger for the more closely situated cations and for the bond angle closer to 180°, the superexchange interaction of A–O–B (J_{AB}) is the strongest, that of B–O–B (J_{BB}) is weaker, and that of A–O–A (J_{AA}) is the weakest. Consequently, the magnetic structure and properties of spinel-type oxides depend strongly on the relative strength of various superexchange interactions among the magnetic moments on A- and B-sites.

As is well known, stoichiometric $ZnFe_2O_4$ crystal possesses a normal spinel structure. This is because there exists a strong tendency for the diamagnetic Zn^{2+} ion to prefer the A-site in oxide crystals with spinel structure. Hence, magnetic Fe^{3+} ions occupy only B-sites, and the negative superexchange interaction among Fe^{3+} ions, J_{BB}, dominates the magnetic properties of $ZnFe_2O_4$. The interaction is weaker because of the 90° angle of Fe^{3+}–O–Fe^{3+}, so $ZnFe_2O_4$ with normal spinel structure is an antiferromagnet with a very low Néel temperature and is paramagnetic at room temperature [3]. Nevertheless, Pavljukhin *et al* [4] reported that the $ZnFe_2O_4$ fine particles derived by mechanical pulverization of bulk $ZnFe_2O_4$ crystal yield high magnetization even at room temperature. Since their report, the unusual high magnetization at room temperature has been realized in $ZnFe_2O_4$ crystal synthesized via different fabrication methods, including a mechanical milling [5], a co-precipitation method [6–8], a rapid quenching method [9–11], and a pulsed-laser-deposition (PLD) technique [12]. Previous studies on co-precipitated nanocrystalline $ZnFe_2O_4$ and rapidly quenched $ZnFe_2O_4$ using extended x-ray absorption fine structure (EXAFS) revealed that Zn^{2+} ions occupy B-sites in addition to the normal A-sites [7, 11]. It is thought that the occupation of B-sites by Zn^{2+} brings about Fe^{3+} ions in both A- and B-sites, and the strong superexchange interaction between Fe^{3+} ions in A- and B-sites, J_{AB}, causes high magnetization at room temperature.

Thin-film fabrication techniques, such as sputtering and PLD, can be utilized to introduce a random distribution of Zn^{2+} and Fe^{3+} in the oxides with spinel structure since they require rapid cooling of vapour phases to form the solid-state phase. However, few studies have been carried out concerning the magnetic properties for the $ZnFe_2O_4$ thin film derived by vapour deposition, so far. Recently, Yamamoto *et al* [12] deposited $ZnFe_2O_4$ thin films on sapphire single-crystal substrate using the PLD technique, and examined the effect of the deposition rate on magnetic properties, keeping the substrate temperature at 500 °C. High magnetization at room temperature is obtained when the thin film is grown at a deposition rate higher than 30 Å min^{-1}, while the thin film accumulated at slower deposition rates such as 7 Å min^{-1} behaves like an antiferromagnet with a magnetic ordering temperature below 20 K, which is similar to the case for $ZnFe_2O_4$ with normal spinel structure. Obviously, the deposition rate is one of the important parameters for controlling the distribution of Zn^{2+} and Fe^{3+} ions in $ZnFe_2O_4$. It is anticipated that the substrate temperature will also have a significant influence on the magnetic properties of $ZnFe_2O_4$, because it determines the cooling rate of vapour phases. The deposition of thin film at lower substrate temperature involves a more rapid cooling process. Hence, one expects low-temperature thin-film processing to be favoured for the formation of the random arrangement of Zn^{2+} and Fe^{3+} in the spinel-type oxides. In addition, establishing the feasibility of inducing high magnetization for $ZnFe_2O_4$ thin films deposited at a low substrate temperature such as room temperature may be useful for commercial fabrication processing, especially in the case where the substrate cannot be heated.

In this paper, we demonstrate that high magnetization at room temperature is readily realized in a $ZnFe_2O_4$ thin film deposited on glass at a substrate temperature close to room temperature, utilizing a sputtering method. Also, the nature of the magnetic ordering in the resultant thin film is investigated by means of measurements of the linear and nonlinear ac susceptibility and dc magnetization. Our results, particularly the nonlinear ac susceptibility measurements, show that the spin freezing behaviour in the present $ZnFe_2O_4$ thin film is similar to that in superparamagnetic systems with intercluster interaction, but is different from that in spin glass systems.

2. Experimental procedure

2.1. Sample preparation and characterization

$ZnFe_2O_4$ thin film was prepared by a radio-frequency sputtering technique (ULVAC RFS-200). Powders of reagent-grade ZnO and Fe_2O_3 were kept at 550 °C for 8 h in air to remove water. The raw materials were weighed so that their molar fraction of 1:1 was attained, and mixed thoroughly. The mixture was compacted and used as a target for sputtering. The thin film was deposited on a commercially available Corning 7059 glass substrate under the following conditions: the rf power was 100 W, the sputtering gas 100% O_2, and the sputtering pressure 27 mTorr. During the film deposition, the substrate was not heated. The thickness of the resultant thin film was evaluated to be 1.06 μm using a surface roughness meter (KLA Tencor, P-15).

The chemical composition of the resultant thin film was analysed using an energy dispersive x-ray spectrometer (EDX, Horiba EMAX-7000). X-ray diffraction (XRD) analysis was performed using Cu Kα radiation (Rigaku RINT2500) in order to identify crystalline phase precipitated in the film. The size of the crystallites was calculated from the full width at half-maximum of the diffraction peaks, and the lattice parameter was estimated from the positions of the diffraction lines.

2.2. dc magnetization and ac susceptibility measurements

Measurements of the dc magnetization and linear ac susceptibility were carried out using a superconducting quantum interference device (SQUID) magnetometer (Quantum Design MPMS2). The dc magnetization as a function of the external magnetic field, $M(H)$, was measured at 5 and 300 K. The dc magnetic field H_{dc} was applied up to 5 T. The temperature dependence of the dc magnetization, $M(T)$, was measured under zero-field-cooled (ZFC) and field-cooled (FC) conditions in the temperature range of 5–350 K. The applied H_{dc} was varied from 20 to 1500 Oe. In the ZFC condition, the sample was cooled in the absence of H_{dc} from room temperature to 5 K, H_{dc} was applied immediately after the temperature of 5 K was reached, and the magnetization data were collected while warming the sample up to 350 K. In the FC operation, the sample was cooled from 350 to 5 K in the presence of H_{dc} while recording the magnetization data. The time dependence of the ZFC magnetization, $M(t)$, was measured at different temperatures between 50 and 300 K. In the measurements, the sample was cooled in the absence of H_{dc} from 350 K to the measured temperatures, and the relaxation of the magnetization was recorded as a function of the elapsed time t after applying $H_{dc} = 100$ Oe. Measurements of the linear ac susceptibility were carried out in the temperature range of 5–350 K. Both in-phase and out-of-phase susceptibilities, $\chi'(T)$ and $\chi''(T)$, were measured at an ac magnetic field $H_{ac} = 3$ Oe and a dc magnetic field $H_{dc} = 50$ Oe. The frequency f of H_{ac} was changed over the wide range of 0.1–1000 Hz. Nonlinear ac susceptibility data

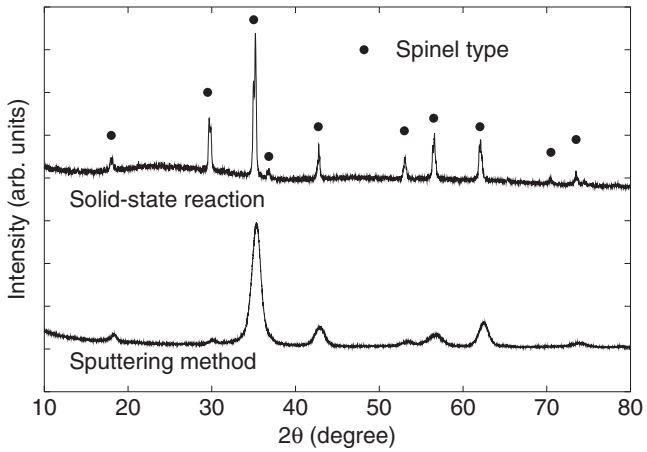

Figure 1. The x-ray diffraction pattern for $ZnFe_2O_4$ thin film derived by a sputtering method. The XRD pattern for bulk $ZnFe_2O_4$ prepared by solid-state reaction is also shown for comparison.

were collected between 5 and 380 K using an ac susceptometer (Quantum Design PPMS). The second- and third-order harmonic components, χ_2 and χ_3, were derived from $2f$ and $3f$ lock-in responses, respectively, using $H_{ac} = 10$ Oe, $H_{dc} = 50$ Oe, and $f = 1000$ Hz.

3. Results

3.1. Analysis of the XRD and chemical composition

Figure 1 shows the XRD pattern for $ZnFe_2O_4$ thin film prepared by a sputtering method. The XRD pattern for polycrystalline $ZnFe_2O_4$ derived from solid-state reaction is also presented for comparison. All the diffraction peaks for the thin film are attributable to the spinel-type $ZnFe_2O_4$, although the width of the peaks is markedly broad compared with that for polycrystal prepared by solid-state reaction. The broadening of the diffraction peaks indicates the smallness of the crystallite size. The crystallite size for the $ZnFe_2O_4$ thin film estimated using Scherrer's equation is approximately 10 nm. The lattice parameter of $ZnFe_2O_4$ with spinel structure precipitated in the thin film was calculated from the positions of diffraction lines corresponding to (311), (400), (422), and (440) planes. The lattice parameter $a(\theta)$ was plotted as a function of the angle of diffraction, θ, and $a(90^\circ)$ was obtained from extrapolation of the lattice parameter to $\theta = 90^\circ$ [13]. We used the least-squares method in the calculation, and evaluated the lattice parameter of $ZnFe_2O_4$ thin film to be 8.431 Å. This value is comparable to or slightly smaller than the lattice parameter of $ZnFe_2O_4$ (franklinite) reported in the JCPDS cards (22-1012), i.e., 8.4385 Å. It should be noted that the lattice constant for the thin film obtained by the sputtering method contains some uncertainties because of the broadness of the diffraction lines. The cation ratio of Zn to Fe in the film was confirmed to be 1.07:2 by EDX measurements; this is close to the ideal ratio for stoichiometric $ZnFe_2O_4$.

3.2. dc magnetization and ac susceptibilities

Magnetizations as a function of the external magnetic field, $M(H)$, are shown at 300 and 5 K for $ZnFe_2O_4$ thin film in figure 2. The $M(H)$ curves tend to be saturated at high magnetic fields. The magnetization at 5 T is as high as 32 emu g^{-1} even at 300 K, and reaches 90 emu g^{-1} at

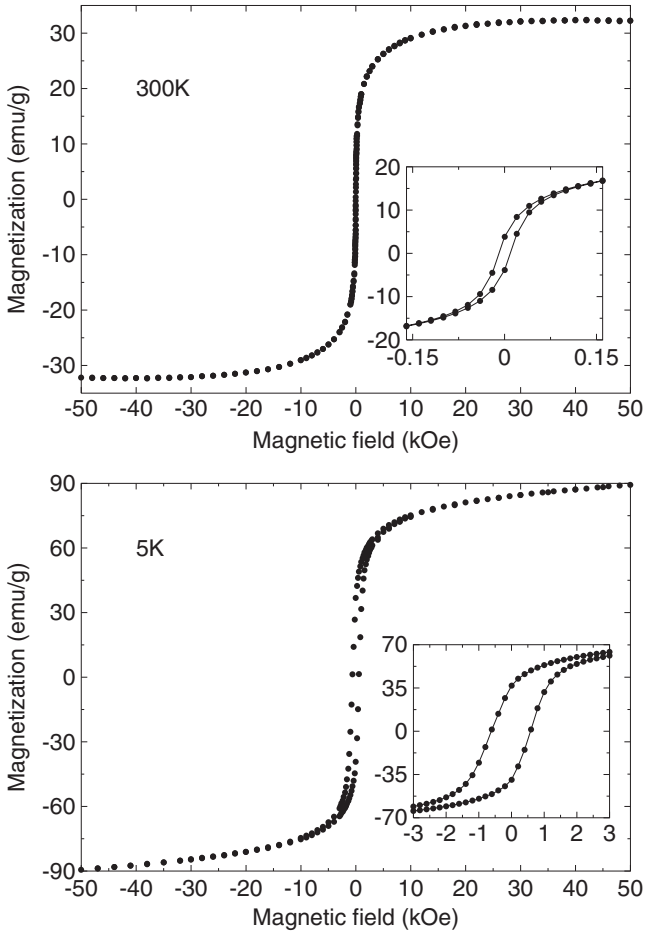

Figure 2. Magnetization as a function of the external magnetic field for $ZnFe_2O_4$ thin film measured at 300 K (upper) and 5 K (lower). The insets enlarge the magnetization curves at low magnetic fields.

5 K. The magnetic hysteresis loops are clearly observed in the low-field ranges, as shown in the insets of figure 2. The hysteresis loop at 5 K is much larger than that at 300 K. Figure 3 shows the temperature dependences of the ZFC and FC magnetizations, $M_{\mathrm{ZFC}}(T)$ and $M_{\mathrm{FC}}(T)$, measured at $H_{\mathrm{dc}} = 20$ Oe. The $M_{\mathrm{ZFC}}(T)$ and $M_{\mathrm{FC}}(T)$ for $H_{\mathrm{dc}} = 50$, 100, 500, and 1500 Oe are also depicted in the inset of figure 3. The $M_{\mathrm{FC}}(T)$ monotonically increases with decreasing temperature, whereas $M_{\mathrm{ZFC}}(T)$ deviates from $M_{\mathrm{FC}}(T)$ below T_{irr}, where $M_{\mathrm{ZFC}}(T)$ and $M_{\mathrm{FC}}(T)$ merge, and exhibits a cusp at T_{max}, where it takes a maximum. As H_{dc} is increased, both the bifurcation temperature T_{irr} and the maximum temperature T_{max} shift to lower temperatures, and the cusp of $M_{\mathrm{ZFC}}(T)$ is broadened.

In figure 4 we show the temperature dependence of the linear ac susceptibility measured at $H_{\mathrm{ac}} = 3$ and $H_{\mathrm{dc}} = 50$ Oe. The upper and lower main frames of figure 4 are the results for in-phase $\chi'(T)$ and out-of-phase $\chi''(T)$ susceptibilities for the frequency $f = 100$ Hz, respectively. Both $\chi'(T)$ and $\chi''(T)$ exhibit broad peaks at around 300 K. As shown in the insets of figure 4, these peaks systematically shift to higher temperature and decrease in height with increase in the frequency of H_{ac}. Nonlinear ac susceptibilities are plotted in figure 5 as

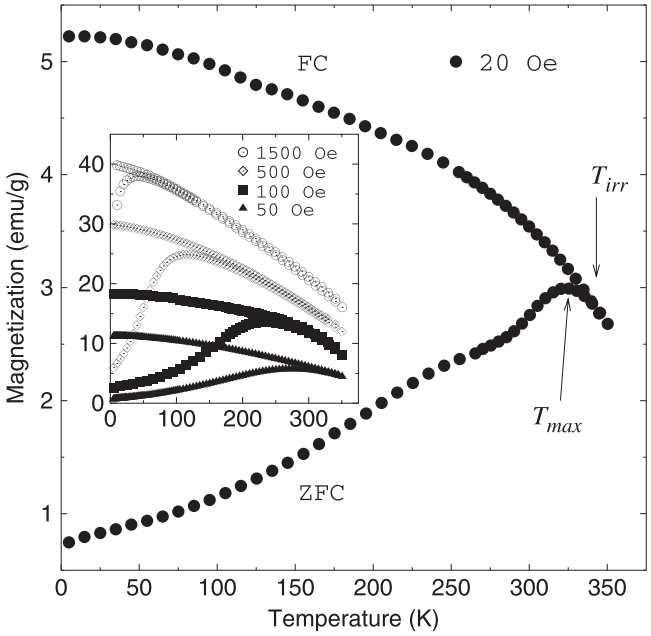

Figure 3. Temperature dependences of ZFC and FC dc magnetizations for $ZnFe_2O_4$ thin film measured at $H_{dc} = 20$ Oe. The inset shows the temperature dependences of ZFC and FC magnetizations measured at $H_{dc} = 50$, 100, 500, and 1500 Oe.

a function of temperature. The upper and lower figures represent temperature variations of the second- and third-harmonic components, $\chi_2(T)$ and $\chi_3(T)$, respectively. Compared to the $\chi'(T)$ and $\chi''(T)$ results, a relatively sharp peak is observed at around 320–340 K in both $\chi_2(T)$ and $\chi_3(T)$. It is seen from figures 3 to 5 that the temperatures of the peaks in the linear and nonlinear ac susceptibilities are close to T_{max} for $M_{ZFC}(T)$ measured at $H_{dc} = 50$ Oe.

Figure 6 shows the time dependence of the ZFC magnetization, $M(t)$, measured after zero-field cooling from 350 K to different temperatures (50, 150, 200, and 250 K) and applying $H_{dc} = 100$ Oe. The ZFC magnetizations manifest a slow nonexponential increase on the timescale as long as 10^4 s. The relaxation of the magnetization strongly depends on the temperature.

4. Discussion

4.1. High magnetization

As mentioned above, the stable phase of $ZnFe_2O_4$ possesses normal spinel structure in which diamagnetic Zn^{2+} and magnetic Fe^{3+} ions are located in the A- and B-sites, respectively. Due to the negative superexchange interaction among Fe^{3+} ions on only B-sites (J_{BB}), the $ZnFe_2O_4$ with normal spinel structure behaves as an antiferromagnet below 10 K and is paramagnetic above this temperature. However, the present $ZnFe_2O_4$ thin film exhibits ferrimagnetic properties and possesses high magnetization even at room temperature, as shown in figure 2. This result clearly indicates that the crystal structure of $ZnFe_2O_4$ thin film is the metastable phase, which is different from the normal spinel structure. A possible mechanism for the observed phenomenon is related to the random arrangement of Zn^{2+} and Fe^{3+} in the spinel-type oxide. In the sputtering method, extremely high energies are imparted to the solid target in

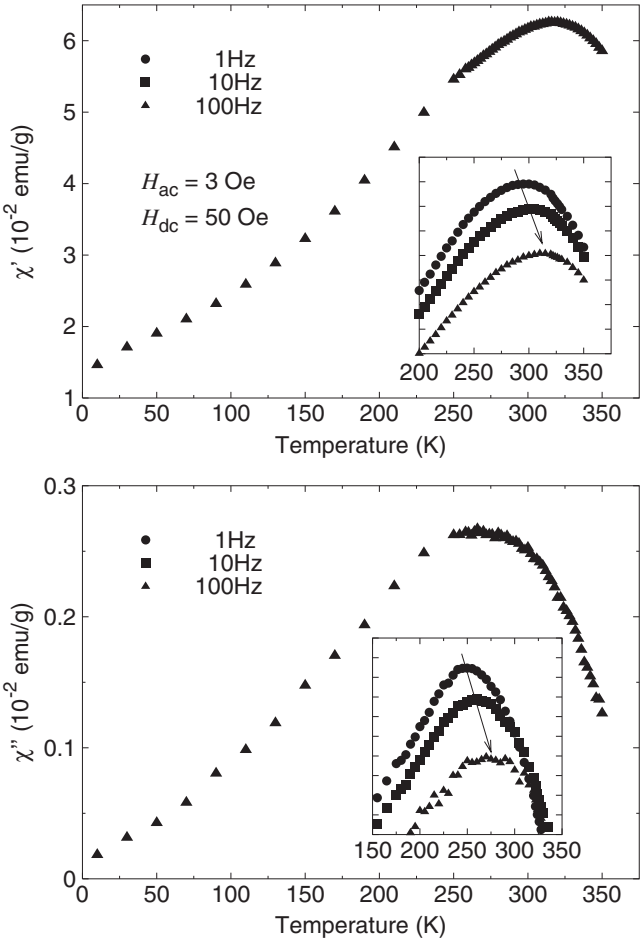

Figure 4. The temperature dependence of the complex ac susceptibility for $ZnFe_2O_4$ thin film measured at $H_{ac} = 3$ Oe and $H_{dc} = 50$ Oe. The upper and lower main frames are the results for the in-phase (χ') and out-of-phase (χ'') components for $f = 100$ Hz, respectively. The upper (lower) inset shows the frequency dependence of the peak in the χ' (χ'') component at around the freezing temperature T_f.

order to obtain highly excited vapour species. Since the resultant vapour phase is very rapidly quenched onto the substrate, the random distribution of Zn^{2+} and Fe^{3+} is frozen as a metastable state. As a result, some of Fe^{3+} ions occupy the A-sites as well as the B-sites, and the presence of strong superexchange interaction between them, J_{AB}, gives rise to the high magnetization at room temperature. As shown in figure 2, the dc magnetization at 5 K reaches about 90 emu g^{-1} at 5 T, which corresponds to the magnetic moment of 1.94 μ_B/Fe ion. Considering the high spin configuration of Fe^{3+} ($3d^5$) and presuming that all the superexchange interactions between A- and B-sites are antiferromagnetic, the cation distribution on A- and B-sites is formulated as $(Zn_{0.39}Fe_{0.61})_A(Zn_{0.61}Fe_{1.39})_BO_4$. This calculation also underlines the assumption that the external magnetic field of 5 T is strong enough to surmount the magnetic anisotropy energy which brings about the misalignment of the summation of magnetic moments among different nanocrystals; that is, all the nanocrystals orient along the direction of the external magnetic field. On the other hand, if the distribution of Zn^{2+} and Fe^{3+} ions in $ZnFe_2O_4$ is completely

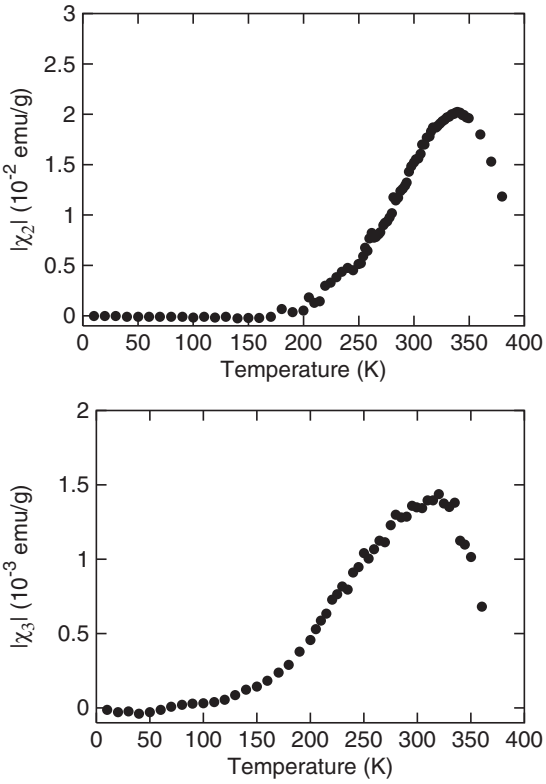

Figure 5. Temperature variations of the nonlinear ac susceptibilities for $ZnFe_2O_4$ thin film measured at $H_{ac} = 10$ Oe, $H_{dc} = 50$ Oe, and $f = 1000$ Hz. The upper and lower frames correspond to second-harmonic (χ_2) and third-harmonic (χ_3) components, respectively.

random, the formula is given by $(Zn_{0.33}Fe_{0.67})_A(Zn_{0.67}Fe_{1.33})_BO_4$. As a result, spinel structure with a highly disordered cationic arrangement is attained in the present thin film, although Zn^{2+} ions slightly prefer A-sites. Very similar behaviour was observed in the $ZnFe_2O_4$ thin film fabricated by the PLD technique [12].

Another mechanism leading to high magnetization at room temperature may be associated with the production of Fe^{2+}. According to previous studies on ZnO–Fe_2O_3 systems prepared by a rapid quenching method [9–11], a solid solution of metastable $ZnFe_2O_4$ and Fe_3O_4 (magnetite) was suggested on the basis of the fact that the lattice parameter of the rapidly quenched zinc ferrite slightly deviates from that of $ZnFe_2O_4$ with normal spinel structure. The magnetite which contributes to the increase in the magnetization was included in the rapidly quenched specimens because of the reduction of Fe^{3+} to Fe^{2+} during the melting at high temperature ($\sim$2000 °C). Such a tendency was particularly prominent in the zinc ferrite with Fe-rich composition. In the present case, however, there is no evidence that the thin film is rich in the Fe element, judging from the EDX compositional analysis. In addition, the optical absorption and the wavelength dependence of the Faraday effect for the thin film indicated no signals due to Fe^{2+} ions in the visible to infrared regions [14]. Furthermore, our recent Zn K-edge EXAFS studies have unambiguously revealed that approximately 60% of Zn^{2+} ions occupy the B-sites in the present thin film [15], which is coincident with that evaluated from the low-temperature $M(H)$ curve as shown in figure 2. Thus, it is reasonable to conclude that

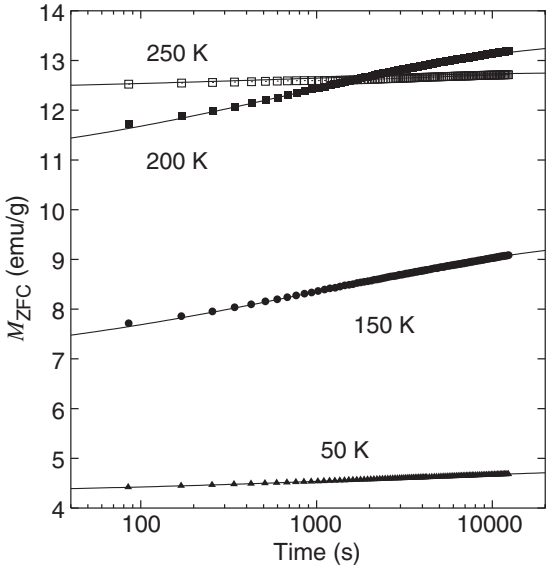

Figure 6. The time dependence of the ZFC magnetization for $ZnFe_2O_4$ thin film measured at 50, 150, 200, and 250 K. The applied dc magnetic field, H_{dc} is 100 Oe. The measurements were performed immediately after zero-field cooling from 350 K. The solid curves represent the best fits of equation (3) to the experimental data.

the main reason for the high magnetization of the present $ZnFe_2O_4$ thin film is not the inclusion of magnetite but mainly the random arrangement of Zn^{2+} and Fe^{3+} in the spinel structure. The details of EXAFS studies will be reported elsewhere.

4.2. Magnetic ordering

In collinear spinel structure, $|J_{AB}| \gg |J_{BB}| \gg |J_{AA}|$ and the system shows long-range ferrimagnetic order [1]. According to the phase diagram proposed by Hubsch *et al* [16] for spinel-type oxides, if the concentration of magnetic ions in A-sites is below 0.33 (percolation limit), the long-range ferrimagnetic order is broken and the magnetic frustration appears on B-sites. The magnetic moments on B-sites are then organized into different sized clusters with short-range antiferromagnetic interactions among clusters. The frustration due to the competition between ferrimagnetic and antiferromagnetic interactions and also the magnetic disorder on B-sites give rise to spin glass-like behaviour in the spinel oxides [17–21]. In such systems, magnetic clusters are formed due to the presence of short-range magnetic ordering at a critical temperature T_c and freeze in random directions below the spin freezing temperature T_f ($<T_c$). It is anticipated that the present $ZnFe_2O_4$ thin film will manifest a spin glass-like phase, because the random distribution of Zn^{2+} and Fe^{3+} ions in the spinel structure results both in frustration due to the competition between J_{AB} and J_{BB} and in randomness owing to the magnetic dilution on B-sites. The superparamagnetic phase is also a very probable magnetic state for the $ZnFe_2O_4$ thin film consisting of an assembly of nanoparticles. We have investigated the nature of magnetic ordering of the $ZnFe_2O_4$ thin film by means of dc magnetization and linear and nonlinear ac susceptibility measurements.

The great discrepancy between $M_{ZFC}(T)$ and $M_{FC}(T)$ below T_{irr} and the shifts of T_{irr} and T_{max} to lower temperatures with increasing H_{dc}, which are shown in figure 3, are indicative of

glassy behaviour. In the canonical spin glass system, the $M_{FC}(T)$ curve below T_{irr} is almost constant [22], while in our data it continues to increase with decreasing temperature, which is usually observed in cluster spin glass materials [23, 24] and also in superparamagnetic particles with dipolar interactions among them [25, 26].

The frequency-dependent peaks in linear ac susceptibilities indicate the slow relaxation processes that characterize the glassy behaviour [22]. As shown in figure 4, the spin freezing in our system occurs at around 300 K as the temperature is lowered from the higher-temperature regime. In $M(T)$ curves shown in figure 3, the spin freezing is indicated by the broad maximum of $M_{ZFC}(T)$. As H_{dc} is decreased, the T_{max} of $M_{ZFC}(T)$ approaches the temperature of the peak of the ac susceptibility, as expected for the freezing of cluster spin glass or superparamagnets. For the lowest $H_{dc} = 20$ Oe used here, the freezing temperature T_f is around 325 K. The high T_f is probably due to the large value of J_{AB} which results from the occupancy of A-sites by Fe^{3+} ions in the spinel structure, since T_f is proportional to the magnitude of the superexchange interaction.

The behaviour of $M(H)$ curves also evidences the absence of long-range ferrimagnetic order. A close look at figure 2 reveals that the magnetization at 5 K is not fully saturated even at 5 T, although the magnetic hysteresis loops are clearly observed in the low-field ranges at 300 K as well as at 5 K. The lack of saturation in the magnetization suggests the presence of antiferromagnetic intercluster interactions in addition to the ferrimagnetic interactions within clusters. This also reflects the canted spin structure inside the clusters [1]. With increasing H_{dc}, the ferrimagnetic part tends to be saturated, while the antiferromagnetic part increases linearly. The antiferromagnetic contribution is pronounced at low temperatures such as 5 K, because the decrease in thermal energy reinforces the intercluster interactions and suppresses the orientation of clusters along the low-magnetic-field directions. On the other hand, the decrease in temperature brings about an increase in the ferrimagnetic contribution as well, as indicated by the larger remanent magnetization and coercivity at 5 K (see the inset of figure 2). This may be attributed to the growth in cluster size, as will be discussed below.

Linear and nonlinear ac susceptibilities have been established as a useful and sensitive tool for investigating the dynamics of the spin freezing phenomenon. Here, we analyse the frequency dependence of $\chi'(T)$ for the present $ZnFe_2O_4$ thin film. The relative shift of the freezing temperature T_f per decade of frequency is $\delta T_f \equiv (\Delta T_f/T_f)/\Delta(\log f) \approx 0.016$ for the present $ZnFe_2O_4$ thin film. For the system of noninteracting magnetic particles, the frequency-dependent peaks in linear ac susceptibilities are characterized by the so-called blocking temperature T_b, and the relative variation of T_b with frequency is of the order of 0.3 [22]. The small δT_f in our case suggests the presence of strong interaction among clusters. The frequency dependence of T_b for the noninteracting particles has been predicted to follow the Arrhenius law:

$$f = f_0 \exp(-E_a/k_B T_b), \tag{1}$$

where f is the driving frequency of H_{ac}, f_0 the frequency factor for the relaxation process, E_a the height of the energy barrier due to magnetic anisotropies, and k_B Boltzmann's constant. As for interacting particle systems, however, deviations from the Arrhenius law take place, and a better fit is obtained using the Vogel–Fulcher law:

$$f = f_0 \exp[-E_a/k_B(T_f - T_0)], \tag{2}$$

where T_0 is a physically unclear parameter but has been regarded as a phenomenological parameter which describes the interactions between particles. Equation (2) indicates a linear dependence of T_f on $1/\ln(f_0/f)$. Figure 7 displays the Vogel–Fulcher plots for the present $ZnFe_2O_4$ thin film, manifesting that our data follow the expected linear behaviour. The parameters obtained by the fitting are $f_0 \approx 10^6$ Hz, $T_0 = 284$ K, and $E_a/k_B = 313$ K. In

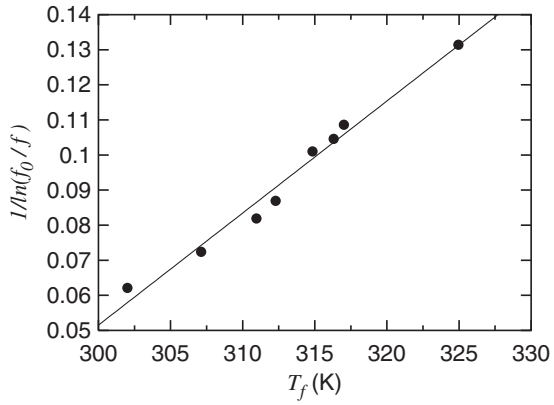

Figure 7. The variation of the spin freezing temperature T_f with the frequency f of the ac field. The solid line represents the Vogel–Fulcher law, i.e., equation (2), fitted to the experimental data. The agreement between the solid line and the data is rather good.

contrast, the Arrhenius law of equation (1) gave a fit with unphysical values of the parameters ($f_0 \sim 10^{45}$ Hz, $E_a/k_B \sim 10^6$ K). The magnetocrystalline anisotropy in spinel-type $ZnFe_2O_4$ crystal is small because Zn^{2+} and Fe^{3+} ions have filled ($3d^{10}$) and half-filled ($3d^5$) electron configurations, respectively. It is thus considered that it is mainly the shape magnetic anisotropy of clusters that induces the energy barrier.

The above-described experimental features can be observed in both the spin glass system and the superparamagnetic system with intercluster interaction. Nonlinear ac susceptibility measurements were performed to distinguish between them. For the spin glass system, a divergence of the third-order nonlinear susceptibility χ_3 takes place at the freezing temperature, signifying a thermodynamic phase transition [22]. In the present system, however, $\chi_3(T)$ exhibits a broad peak at around the freezing temperature T_f (∼325 K), as shown in figure 5. Similar behaviour was experimentally observed in fine-particle systems [27–29] and could be theoretically explained within the framework of Wohlfarth's superparamagnetic blocking model [30]. When H_{dc} is present in addition to the driving H_{ac}, second-order nonlinear susceptibility χ_2 can be induced through a $\chi_2 = \chi_3 H_{dc}$ process if higher harmonic components are neglected. As a result, the broad peak in $\chi_2(T)$ also provides proof that the spin freezing is not caused by the spin glass transition but by the progressive freezing of superparamagnetic clusters. Thus, the broad peaks in $\chi_2(T)$ and $\chi_3(T)$, as well as the weakly frequency-dependent peak in $\chi'(T)$, allow us to infer superparamagnetism with interaction among magnetic clusters.

In order to obtain further information on the underlying nature of the superparamagnetic system with intercluster interaction, we have investigated the time-dependent relaxation of the ZFC magnetization at $H_{dc} = 100$ Oe. The increase in magnetization with time, as shown in figure 6, means that magnetic clusters gradually reorient to a more stable state in the direction of an external magnetic field. The long-time relaxation of the ZFC magnetization indicates the existence of a metastable magnetic state. Among the various functional forms that have been proposed for describing long-time relaxation, an empirical stretched exponential is the most popular. Here, the time evolution of the magnetization is analysed using a combination of a stretched exponential and a constant term:

$$M(t) = M_0 - M_r \exp[(-t/\tau)^\beta], \tag{3}$$

where M_0 and M_r are the constants, and τ the characteristic time constant. M_0 represents an intrinsic ferrimagnetic component, and M_r is related to a glassy component contributing to

Table 1. Parameters used to fit equation (3) to the relaxation of the ZFC magnetization.

T (K)	M_0 (emu g^{-1})	M_r (emu g^{-1})	β	τ (10^3 s)
250	12.8	0.38	0.35	0.60
200	13.38	2.79	0.35	0.88
150	9.44	2.15	0.31	1.24
50	4.80	0.53	0.31	3.21

the relaxation. The solid curves of figure 6 show the relaxation functions of equation (3) with the parameters listed in table 1. The agreement between equation (3) and our experimental data is rather good. The values of β lie in the range 0.3–0.35 and are almost independent of temperature. On the other hand, the parameters M_0, M_r, and τ depend substantially on the temperature. As the temperature is decreased, M_0 and M_r increase, take a maximum around 200 K, and then decrease. The maximum temperature is very close to the cluster freezing temperature T_f as indicated by the maximum of $M_{ZFC}(T)$ at $H_{dc} = 100$ Oe (see the inset of figure 3). The similar temperature variations of M_0 and M_r support the idea that the finite-range ferrimagnetic ordering is responsible for the formation of spatially confined clusters. As the temperature is decreased toward and below the freezing temperature, the intracluster and intercluster interactions become more effective, and the sizes of clusters rapidly increase. Larger clusters give rise to a slower response time, or longer relaxation time (τ), due to larger free-energy barriers; the smaller the clusters become, the more rapidly they relax. The glassy component M_r thus increases down to 200 K as a result of the growth of the cluster size. In contrast, M_r becomes smaller as the temperature is further lowered below 200 K, because the cluster growth eventually leads to the freezing of the clusters below T_f. It is conceivable that the significant interactions among the oversized clusters dominate the magnetic relaxation behaviour at low temperatures well below T_f.

The overall experimental data presented here demonstrate that the highly disordered arrangement of Zn^{2+} and Fe^{3+} in $ZnFe_2O_4$ thin film derived by the sputtering method brings about an unusual magnetic state with the coexistence of phenomena related to ferrimagnetic ordering and magnetic glassy behaviour. The presence of ferrimagnetic ordering is evidenced by the magnetic hysteresis loop in the $M(H)$ curves, and the increase in $M_{FC}(T)$ below T_{irr}. On the other hand, the great discrepancy between $M_{ZFC}(T)$ and $M_{FC}(T)$ below T_{irr}, the frequency-dependent peak of the linear ac susceptibility, the occurrence of the peak in the nonlinear ac susceptibility, and the long-time relaxation of the ZFC magnetization are indications of glassy behaviour. These results suggest that an infinite or percolating ferrimagnetic network, as expected for the spinel-type oxides in which the strong superexchange interaction J_{AB} is predominant [1], is broken into discrete, but yet strongly interacting clusters.

5. Conclusions

$ZnFe_2O_4$ thin film was deposited on glass substrate at a low substrate temperature close to room temperature using a sputtering method, and the nature of the magnetic ordering was clarified using dc magnetization and ac susceptibility measurements. XRD analysis indicates that the thin film is single-phase $ZnFe_2O_4$. EDX data confirm that the chemical composition of the thin film is close to the ideal value of $ZnFe_2O_4$. The present $ZnFe_2O_4$ thin film manifests ferrimagnetic behaviour and possesses magnetization as high as 32 emu g^{-1} at 5 T even at room temperature. We ascribed the unusual high magnetization to the occupation of the A-sites by Fe^{3+} ions accompanied with Zn^{2+} ions in the B-sites. The lack of magnetic saturation in the $M(H)$ curves at low temperatures, the great discrepancy between $M_{ZFC}(T)$ and $M_{FC}(T)$ below

T_{irr}, the frequency-dependent peak in the linear ac susceptibility, and the broad peak in the nonlinear susceptibility demonstrate the glassy behaviour and the absence of true long-range ferrimagnetic order. The frequency dependence of the freezing temperature follows the Vogel–Fulcher law, implying the presence of magnetically interacting clusters. The relaxation of the ZFC magnetization at various temperatures is well described on the basis of an empirical stretched exponential relation and can be interpreted using a model in which ferrimagnetic clusters grow with decreasing temperature. These overall results suggest that the magnetic state of this material is superparamagnetic with finite-range ferrimagnetic order within clusters and with interactions among clusters. The curious magnetic state in the present $ZnFe_2O_4$ thin film is presumably caused by highly disordered arrangements of Zn^{2+} and Fe^{3+} in the spinel structure.

Acknowledgments

The authors thank Dr Masaki Azuma of the Institute of Chemical Research, Kyoto University, for the nonlinear ac susceptibility measurements. This work was carried out under the Nanotechnology Glass Project as part of the Nanotechnology Materials Programme, which is financially supported by the New Energy and Industrial Technology Development Organization (NEDO), Japan. Part of this work was also supported by a Grand-in-Aid for Exploratory Research from the Ministry of Education, Culture, Sports, Science, and Technology, Japan.

References

[1] Dormann J L and Nogues M 1990 *J. Phys.: Condens. Matter* **2** 1223
[2] Villain J 1979 *Z. Phys.* B **33** 31
[3] Pettit G A and Forester D W 1971 *Phys. Rev.* B **4** 3912
[4] Pavljukhin Yu T, Medikov Ya Ya and Boldyrev V V 1983 *Mater. Res. Bull.* **18** 1317
[5] Chinnasamy C N, Narayanasamy A, Ponpandian N, Chattopadhyay K, Guerault H and Greneche J-M 2000 *J. Phys.: Condens. Matter* **12** 7795
[6] Kamiyama T, Haneda K, Sato T, Ikeda S and Asano H 1992 *Solid State Commun.* **81** 5
[7] Jeyadevan B, Tohji K and Nakatsuka K 1994 *J. Appl. Phys.* **76** 6325
[8] Sato T, Haneda K, Seki M and Iijima T 1990 *Appl. Phys.* A **50** 13
[9] Tanaka K, Nakahara Y, Hirao K and Soga N 1994 *J. Magn. Magn. Mater.* **131** 120
[10] Tanaka K, Makita M, Hirao K and Soga N 1998 *J. Magn. Soc. Japan* **22** (Suppl. S1) 77
[11] Tanaka K, Makita M, Hirao K and Soga N 1998 *J. Phys. Chem. Solids* **59** 1611
[12] Yamamoto Y, Tanaka H and Kawai T 2001 *Japan. J. Appl. Phys.* **40** L545
[13] Nelson J B and Riley D P 1945 *Proc. Phys. Soc.* **57** 160
[14] Tanaka K, Nakashima S, Fujita K and Hirao K 2003 *J. Phys.: Condens. Matter* **15** L469
[15] Nakashima S, Fujita K, Tanaka K, Hirao K, Yamamoto T and Tanaka I 2004 in preparation
[16] Hubsch J, Gavoille G and Bolfa J 1978 *J. Appl. Phys.* **49** 1363
[17] Fiorani D, Viticoli S, Dormann J L, Tholence J L and Murani A P 1984 *Phys. Rev.* B **30** 2776
[18] Brand R A, Georges-Gibert H, Hubsch J and Heller J A 1985 *J. Phys. F: Met. Phys.* **15** 1987
[19] Sing R and Bhargava S C 1995 *J. Phys.: Condens. Matter* **7** 8183
[20] Bhargava S C, Morrish A H and Kunkel H 2000 *J. Phys.: Condens. Matter* **12** 9667
[21] Bhowmik R N and Ranganathan R 2002 *J. Magn. Magn. Mater.* **248** 101
[22] Mydosh J A 1993 *Spin Glasses: An Experimental Introduction* (London: Taylor and Francis)
[23] Itoh M, Natori I, Kubota S and Motoya K 1994 *J. Phys. Soc. Japan* **63** 1486
[24] Mukherjee S, Ranganathan R, Anilkumar P S and Joy P A 1996 *Phys. Rev.* B **54** 9267
[25] Luo W, Nagel S R, Rosenbaum T F and Rosenweig R E 1991 *Phys. Rev. Lett.* **67** 2721
[26] Garcia J L, Lopez A, Lazaro F J and Martinez C 1996 *J. Magn. Magn. Mater.* **157/158** 272
[27] Bitoh T, Ohba K, Takamatsu M, Shirane T and Chikazawa S 1996 *J. Magn. Magn. Mater.* **154** 59
[28] Bajpai A and Banerjee A 2000 *Phys. Rev.* B **62** 8996
[29] Jönsson P, Jonsson T, Garcia-Palacios J L and Svedlindh P 2000 *J. Magn. Magn. Mater.* **222** 219
[30] Wohlfarth E P 1979 *Phys. Lett.* A **70** 489